New Journal of Physics
The open access journal at the forefront of physics
Deutsche Physikalische Gesellschaft DPG IOP Institute of Physics

OPEN ACCESS

Bifurcations and safe regions in open Hamiltonians

To cite this article: R Barrio *et al* 2009 *New J. Phys.* **11** 053004

View the article online for updates and enhancements.

You may also like

- On the existence of a new type of periodic and quasi-periodic orbits for twist maps of the torus
Salvador Addas-Zanata
- Symbolic dynamics and periodic orbits of the Lorenz attractor*
Divakar Viswanath
- Periodic orbits around areostationary points in the Martian gravity field
Xiao-Dong Liu, Hexi Baoyin and Xing-Rui Ma

This content was downloaded from IP address 3.142.96.146 on 29/04/2024 at 14:12

New Journal of Physics
The open-access journal for physics

Bifurcations and safe regions in open Hamiltonians

R Barrio[1,3], **F Blesa**[2] **and S Serrano**[1]
[1] GME, Dpto Matemática Aplicada and IUMA, Universidad de Zaragoza, E-50009 Zaragoza, Spain
[2] GME, Dpto Física Aplicada, Universidad de Zaragoza, E-50009 Zaragoza, Spain
E-mail: rbarrio@unizar.es, fblesa@unizar.es and sserrano@unizar.es

New Journal of Physics **11** (2009) 053004 (15pp)
Received 19 January 2009
Published 19 May 2009
Online at http://www.njp.org/
doi:10.1088/1367-2630/11/5/053004

Abstract. By using different recent state-of-the-art numerical techniques, such as the OFLI2 chaos indicator and a systematic search of symmetric periodic orbits, we get an insight into the dynamics of open Hamiltonians. We have found that this kind of system has safe bounded regular regions inside the escape region that have significant size and that can be located with precision. Therefore, it is possible to find regions of nonzero measure with stable periodic or quasi-periodic orbits far from the last KAM tori and far from the escape energy. This finding has been possible after a careful combination of a precise 'skeleton' of periodic orbits and a 2D plate of the OFLI2 chaos indicator to locate saddle-node bifurcations and the regular regions near them. Besides, these two techniques permit one to classify the different kinds of orbits that appear in Hamiltonian systems with escapes and provide information about the bifurcations of the families of periodic orbits, obtaining special cases of bifurcations for the different symmetries of the systems. Moreover, the skeleton of periodic orbits also gives the organizing set of the escape basin's geometry. As a paradigmatic example, we study in detail the Hénon–Heiles Hamiltonian, and more briefly the Barbanis potential and a galactic Hamiltonian.

[3] Author to whom any correspondence should be addressed.

 © IOP Publishing Ltd and Deutsche Physikalische Gesellschaft

Contents

1. Introduction

In the past few years the interest in the study of open Hamiltonians has been growing [1]–[3], looking at particular properties of the fractal exit basins and locating the chaotic regions. These studies have applications in several applied fields such as plasma physics [4], modeling the dynamics of ions in electromagnetic traps [5], computational chemistry (by instance, in [6] the example chosen to apply the transition state theory for laser-driven reactions is a driven Hénon–Heiles (HH) system and the Barbanis potential is extensively used in quantum dynamics [7] and to model fluorescence excitation of benzophenone [8]), and so on.

In this paper, we are interested in studying the dynamics of open Hamiltonians. When the energy of these systems goes beyond the escape energy most of the orbits escape, and in the Hamiltonians we study, as there are several exits, it is possible that a test particle escapes through any of them. As a test example, we have chosen first to study the paradigmatic HH Hamiltonian [9]. Note that this system has received much attention in the last few years establishing, for instance, some results on cascades of pitchfork bifurcations [10]–[12] or studying in detail the fractal structures in the regular and escape regions [3, 13]. In order to generalize the results, we have also carried out a short analysis of two other open Hamiltonians with two and four exits [14].

The main goal of the present paper is to obtain new results on these systems by using some new techniques for the study of 2DOF Hamiltonian systems, which permit us to analyze them in much more detail. We combine the use of a fast chaos indicator (OFLI2) [15, 16] to indicate regular regions on the (y, E) plane and a systematic search of symmetric periodic orbits [17]–[22] that permits us to obtain with great precision the 'skeleton' of periodic orbits of the system. Both techniques provide complementary results, which permit one to state the existence of bounded stable regular regions of a significant size and located with precision inside the escape region. These regions are far from the KAM regime; therefore, they are quite interesting as they provide safe bounded regular regions inside the escape region. Note that it is well known that undoubtedly hyperbolic systems are unlikely to exist and that everywhere in parameter space of bounded systems there may be stability islands [23] after the KAM tori disappear but of extremely small size and extremely difficult to locate. Therefore, a precise location of bounded stable regions permits their use in practical applications because they may serve as safe regions in the 'escape sea'. Besides, we show how the normal modes Π_i and the skeleton of periodic orbits configure the geometry of the exit basins of any problem of this kind.

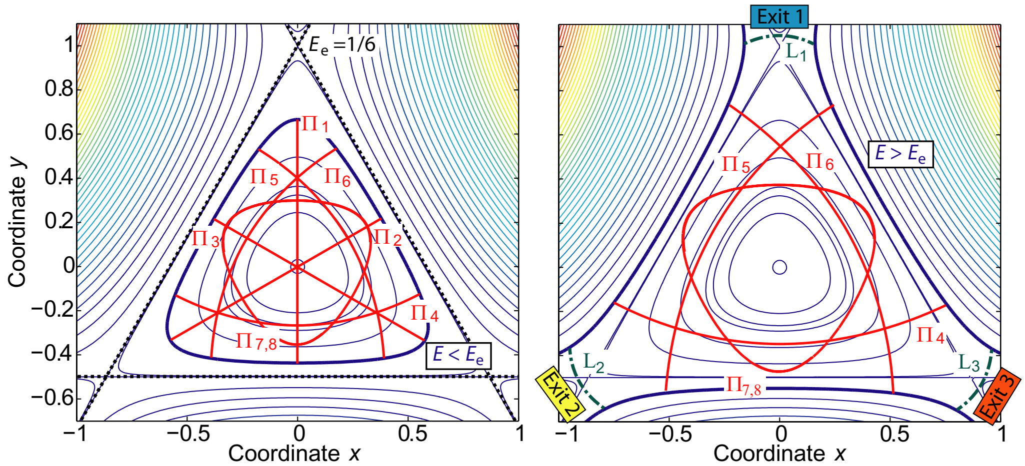

Figure 1. Level curves of the HH potential, exits, limit of bounded motion, and the eight Π_i nonlinear normal modes on the (x, y) plane for $E < E_e$ (on the left) and $E > E_e$ (on the right).

The organization of the paper is as follows. In section 2 we describe how to classify the orbits according to type. In section 3 we obtain the skeleton of periodic orbits, and in section 4 we show several interesting bifurcations of the HH Hamiltonian. In section 5 we perform a short analysis for other open Hamiltonians. Finally, we present some conclusions.

2. Types of orbits: regular, chaotic and escape

We plan to explore the types of orbits that appear on open Hamiltonians. To do so we fix initially as our test problem the most famous open Hamiltonian, the classical [9] HH Hamiltonian, which is given by

$$\mathcal{H} = \tfrac{1}{2}(X^2 + Y^2) + \tfrac{1}{2}(x^2 + y^2) + \left(yx^2 - \tfrac{1}{3}y^3\right). \tag{1}$$

The HH system presents different symmetries, its complete symmetry group being $D_3 \times \mathcal{T}$ (D_3 is a dihedral group and $\mathcal{T}$ is a $\mathbb{Z}_2$ symmetry, the time-reversal symmetry). This Hamiltonian has attracted a large number of researchers and in the past few years more papers have appeared [2, 13], [24]–[28]. It has been studied mainly for energy values below the *escape energy* $E_e = 1/6$ (for energy values below E_e the level curves are closed and all the orbits are bounded, exhibiting chaotic or regular motion, whereas the equipotential lines corresponding to the escape energy form an equilateral triangle, and for higher values the vertices of the triangle open and most of the orbits are unbounded escape orbits). Due to the D_3 symmetry of the system, there are three exits [1, 2]: Exit 1 ($y \to +\infty$), Exit 2 ($y \to -\infty, x \to -\infty$) and Exit 3 ($y \to -\infty, x \to +\infty$). For energies greater than E_e, there exist three orbits L_i, known as Lyapunov orbits, one corresponding to each exit, which act as frontiers: any orbit that crosses them with an outward-oriented velocity must go to infinity.

In figure 1 we show a scheme of the level potential curves, the three exits, and the eight nonlinear normal modes Π_i for energy values $E < E_e$ and $E > E_e$ (note that from Weinstein's theorem [29] there are at least two and due to the D_3 symmetry there are eight [30]). These nonlinear normal modes are described (using the terminology of Churchill *et al* [30]) as follows: the projections of the $\Pi_{1,2,3}$ orbits lie on the gradient lines of the potential that passes through the origin, and they are directed towards Exits 1, 2 or 3. Therefore, $\Pi_{1,2,3}$ orbits disappear at the escape energy, when the Lyapunov orbits L_i appear. The projections are symmetric with respect to the D_3 group. The $\Pi_{4,5,6}$ orbits start at a point with a given energy E and intersect the gradient line Π_{i-3} perpendicularly. Finally, Π_7 is a periodic orbit whose trajectory is counterclockwise forming perpendicular intersections with all three gradient lines $\Pi_{1,2,3}$. Due to the $\mathcal{T}$ symmetry, Π_8 coincides with Π_7, but it goes clockwise.

Now, focusing on our goal of classifying the orbits we use two methods. On the one hand, we study the problem with a chaos indicator. This allows us to determine the regular and chaotic regions that appear in the problem. On the other hand, we propagate the initial conditions and we study if they give rise to escape or bounded orbits. This will permit us to obtain the exit basins and to study their character. We use both methods to complement each other.

First, we analyze the regular and chaotic regions using OFLI2 [15, 16], which is a fast chaos indicator. It detects the set of initial conditions where we may expect sensitive dependence on initial conditions. The value of the OFLI2 indicator at the final time t_f is given by

$$\mathrm{OFLI2} := \sup_{0<t<t_\mathrm{f}} \ln \|\{\boldsymbol{\xi}(t) + \tfrac{1}{2}\,\delta\boldsymbol{\xi}(t)\}^{\perp}\|, \tag{2}$$

where $\boldsymbol{\xi}$ and $\delta\boldsymbol{\xi}$ are the first- and second-order sensitivities with respect to carefully chosen initial vectors, and $\boldsymbol{x}^{\perp}$ represents the orthogonal component to the flow of the vector $\boldsymbol{x}$. See [15, 16] for a complete description of the method. All the numerical calculations are done using a variable-stepsize, variable-order extended Taylor series method [31]. In the OFLI2 plots of figure 2, orange coincides with the more regular regions, whereas white denotes chaos (note that above the escape energy, black and white denote escape orbits without and with transient chaos, respectively).

In figure 2, we show three OFLI2 plots. Plots A and B are drawn on the (y, E) plane and plot C on the (x, E) plane. Plots A and C show that the regular behavior appears mainly below the escape energy. As the energy approaches the escape value E_e, the chaotic behavior increases. Above that value the escape region increases but there are transient chaos zones corresponding to the fractal boundaries. A very interesting fact of the studied open Hamiltonians is that it is also possible to find small regular regions far from the KAM regime (the last KAM torus disappears on the y-axis around $E \simeq 0.2113$ (plot A)), as shown by the magnification plot B. These regular and bounded regions placed far from the escape energy (as in plot B) are generated from saddle-node bifurcations of periodic orbits. Therefore, it is possible to find regions of nonzero measure with stable periodic or quasi-periodic orbits far from the last KAM tori and far from the escape energy. So, these regions act as safe bounded regular regions inside the escape region, giving the only initial conditions of these systems that exhibit this behavior for large values of the energy. For energy values greater than $E \simeq 0.27$, the escape regions dominate and the saddle-node generation stops.

Now we compare with the information given by the exit basins. As already known, the exit basin [1, 3, 32] of a particular exit is the set of initial conditions that yield escape through such an exit. As expected, the geometry of the exit basins is fractal [3]. In [13], we calculated its fat-fractal exponent. In figure 2, we show the exit basins on the (y, E) plane by fixing $x = Y = 0$. The color codes for the exit basins are as follows: green—bounded motion, blue—Exit 1, yellow—Exit 2, and red—Exit 3. We observe a simplification of the geometry as the energy grows, giving an asymptotic band structure as shown in plot D. The structure becomes simpler with sharper bounds; therefore, we expect the fat-fractal exponent to increase.

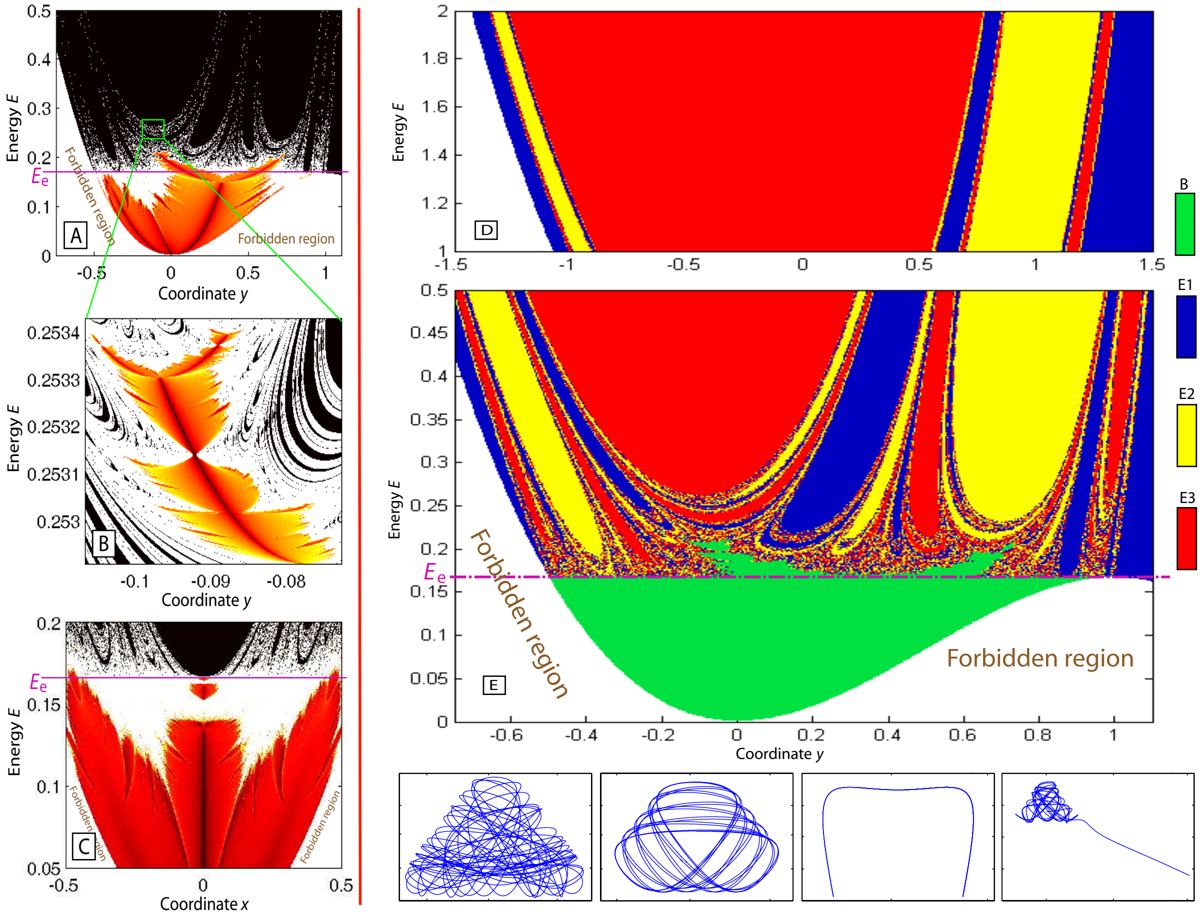

Figure 2. Left: (A) OFLI2 plot on the (y, E) plane, (B) magnification of a bounded region and (C) OFLI2 plot on the (x, E) plane around Π_1. Orange or black color indicates regular movement (bounded or escape) and white color corresponds to chaotic areas. Right: (E) exit basins on the (y, E) plane. (D) shows the behavior of the exits for large values of the energy. Bottom right: different types of orbits (from left to right: a KAM orbit in the bounded region, two periodic orbits with D_3 or time-reversal symmetry and an escape orbit).

On the bottom right part of figure 2, we have plotted from left to right several examples of the kinds of orbits that may appear in this problem: a KAM orbit, a periodic orbit with D_3 symmetry, a periodic orbit without D_3 symmetry but with time-reversal symmetry and an escape orbit through Exit 3 after a transient phase.

3. Skeleton of periodic orbits

Once we have located the regions with different behavior, we look for invariants of the systems that configure the regions. In our case, the invariants are families of symmetric periodic orbits (s.p.o.), and so we look for a complete skeleton of s.p.o.

We have used a systematic search method [17, 28] that allows an easy detection of s.p.o. for 2DOF Hamiltonian systems with some symmetries. The origin of the method is quite old; in fact it was introduced by Birkhoff [18], DeVogelaere [20], Hénon [21, 22] and Strömgren [19] (among others) and used to find s.p.o. An updating of the method is described in detail in [17] (and references therein), but for completeness it can be summarized as follows. The HH system is symmetric with respect to the variable x and it is time-reversible. If $\{x(t), y(t)\}$ is a solution, then $\{-x(-t), y(-t)\}$ is also a solution. Therefore, if an orbit starts at the y-axis perpendicular to it,

$$(x(0), y(0), X(0), Y(0)) = (0,\ y_0,\ X_0, 0), \tag{3}$$

and crosses again the y-axis perpendicularly, then the orbit is closed and symmetric and so it is a symmetric periodic orbit with period T (twice the crossing time). Therefore the condition for a symmetric periodic orbit is

$$x(0, y_0, X_0, 0;\ T/2) = Y(0, y_0, X_0, 0;\ T/2) = 0. \tag{4}$$

Since the symmetric periodic orbit could have a multiplicity m greater than one, we look for the crossing conditions after m crossings of the y-axis. According to these symmetry conditions, we choose for the Poincaré map the plane y–Y (with $x = 0$, so we compute X from the energy). To find the crossing conditions, we perform a mesh on the E or y plane and look for the changes of sign of Y at the crossings. So we need two root-finding processes.

Once a symmetric periodic orbit has been calculated, we analyze the stability of the orbit. The linear stability is studied by means of the eigenvalues of the monodromy matrix $\Pi(T)$, that is, the solution at time T (one period of the periodic orbit) of the matrix linear differential system given by the first-order variational equations. For a periodic orbit in a Hamiltonian system we always have two eigenvalues equal to one, corresponding to perturbations along the periodic orbit and perpendicular to the energy shell on the phase space T^*Q_2. In fact, we just need the trace of the monodromy matrix, which is the sum of the diagonal elements, and it is therefore equal to the sum of the eigenvalues. Following Hénon [21, 22] we use instead the trace minus two defining the *stability index* $\kappa := \kappa(\Pi(T)) = \mathrm{Tr}\,(\Pi(T)) - 2$. Thus a periodic orbit is linearly stable (elliptic periodic orbit) iff $|\kappa| < 2$, unstable iff $|\kappa| > 2$ and critical iff $|\kappa| = 2$.

According to Meyer [33], an elementary periodic solution (i.e. with $\kappa \neq 2$) in a system depending on a parameter $\mathcal{P}$ with a non-degenerate integral can be continued when the parameter is changed. Therefore, for autonomous Hamiltonian systems the periodic orbits appear in *families*. Note that if we have a non-elementary periodic solution the periodic orbit may appear or disappear. A family of periodic orbits is represented by a continuous curve (the *characteristic curve*) in the plane of initial conditions or parameters. We use the energy E as the parameter $\mathcal{P}$ to be continued.

In figure 3, we show a joint OFLI2 and s.p.o. plot on the (y, E) plane. Note that in such a plot any point corresponds to the initial conditions of one orbit. We can see how both techniques complement each other. Each figure consists of a regular grid of 1000×1000 points (10^6 orbits) and we have used double precision with an error tolerance $\mathrm{Tol} = 10^{-14}$. In figures A, C and E, we have used a color code for the different multiplicities of the periodic orbits. In plot A, we show the s.p.o. $(x(0) = Y(0) = 0)$ versus the energy constant E up to multiplicity $m = 5$. In plots B, D and F, we show the stability of the orbits (in green the stable and in red the unstable ones). Plots C and D show the region below the escape energy, but now up to multiplicities $m = 12$. The forbidden region is located outside the thick black line. Plots E and F present a regular region well above the escape energy E_e. It corresponds to plot B of figure 2.

We note the presence of the families of the normal modes $\Pi_{4,7,8}$ (the black lines originating at $E = 0$) that configure the behavior for large E as the other families of periodic orbits

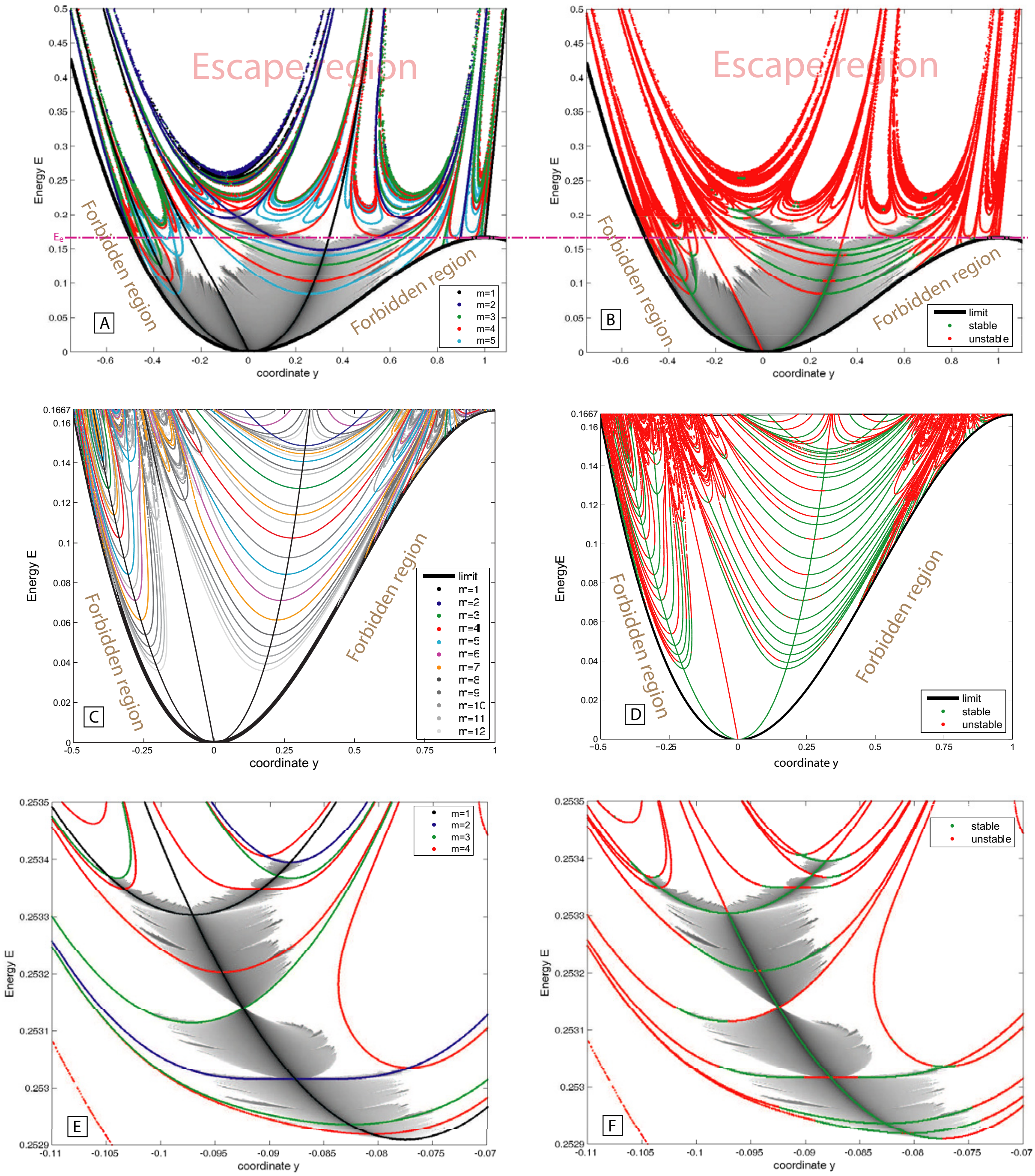

Figure 3. OFLI2 plots of regular bounded regions (on gray scale, black lines being the location of the periodic orbits) on the (y, E) plane and superposed the skeleton of s.p.o. (on plates A, C and E for different multiplicities shown in the color legend and on plates B, D and F in green the stable orbits and in red the unstable ones).

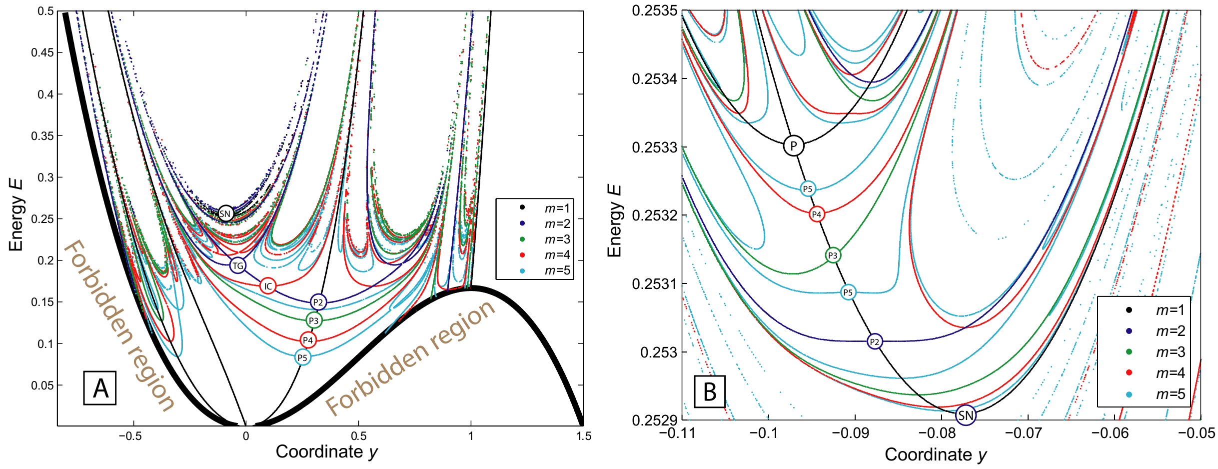

Figure 4. Bifurcations of the families of s.p.o. of different regions of the (y, E) plane. Plot B is a zoom of the SN zone in plot A. The families of s.p.o. are drawn in different colors according to their multiplicity up to $m = 5$ and the code for the bifurcations is SN—saddle-node, TG—touch-and-go, IC—tripled 2-period island chain and Pm stands for an m-multiplicity bifurcation.

accumulate around them and define the boundaries of the exit basins (compare figures 2(A), 2(E) and 3(A)).

4. Bifurcations

When we have a family of periodic orbits we are interested in knowing when it appears, disappears or bifurcates. If $\kappa \neq 2$ then a periodic orbit is a member of a smooth one-parameter family of periodic orbits. Moreover, the converse gives quite an important result: periodic orbits can only appear or disappear when their stability index is $\kappa = 2$. Therefore [17], a periodic orbit of multiplicity m (or a subharmonic bifurcation) can appear or disappear at points of the main periodic orbit (m-bifurcation points) such that

$$\kappa = 2\cos(2\pi k/m), \qquad k < m \tag{5}$$

with k and m coprime natural numbers (note that the bifurcated orbit will have $\kappa = 2$). The ratio k/m is called the rotation or winding number. At this point the main periodic orbit bifurcates in periodic orbits of multiplicity m. This can only happen when the main p.o. is stable or critical $|\kappa| \leqslant 2$.

Figure 4 shows several subharmonic bifurcations on the plot of families of s.p.o. up to multiplicity $m = 5$. Each color corresponds to a different multiplicity. Plot B is a zoom of the region marked as SN in plot A. In plot A, we indicate with labels some bifurcations explained later with greater detail in figure 6. In plot B we do the same thing with bifurcations of figure 5. There is good agreement with the expected values according to equation (5). Note that Meyer's classification of generic bifurcations is not enough for systems with symmetry. The generic bifurcations are the only typical bifurcations [33] after a family of periodic orbits has lost all the symmetries. Other bifurcations can occur only in the presence of symmetries and involve a loss of some symmetries in the new families of periodic orbits. Kurosaki [34] and Ozakin and

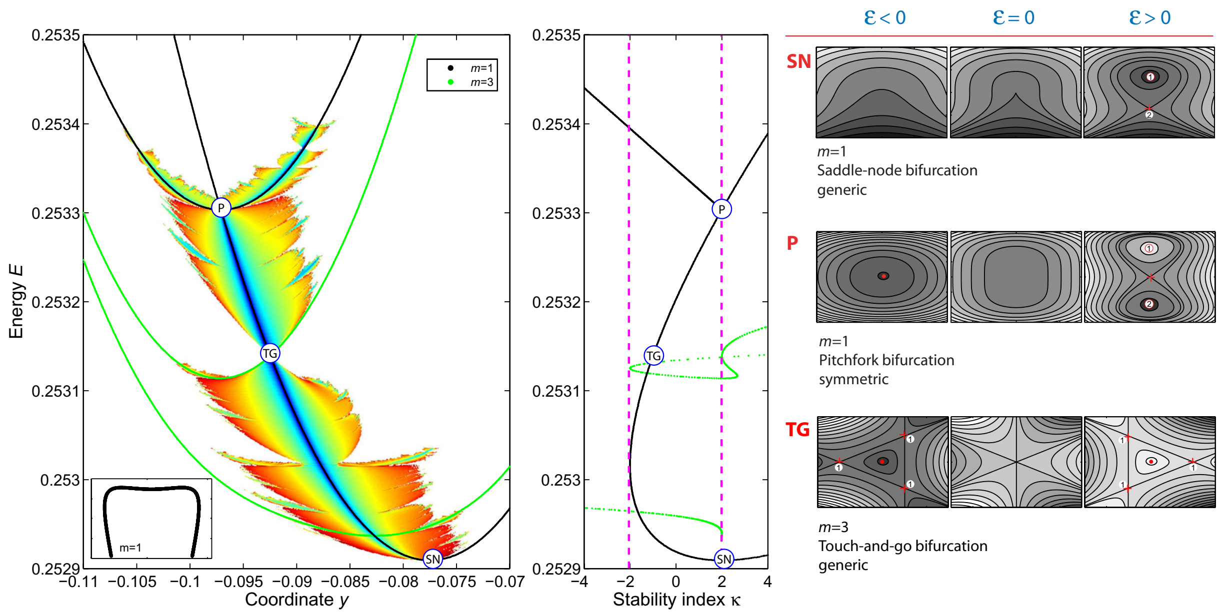

Figure 5. Generic and y-axis symmetric bifurcations in a regular region above the escape energy. On the left, both OFLI2 and families of periodic orbits. The middle plot shows the stability index κ of these families. The multiplicity $m = 1$ orbit shown on the left is created at the SN bifurcation and has no D_3 symmetry. On the right, schematic Poincaré surface sections.

Kurosaki [35] also found some of these bifurcations for values of nonlinear modes below the escape energy. From the skeleton of s.p.o. on plot B, we observe that this regular and bounded region originates from the stable branch of s.p.o. coming from a saddle-node bifurcation. It continues until a pitchfork bifurcation is found. If we continue the stable branch, on the right, a period-doubling bifurcation appears (in blue in picture 3(E)) around energy $E = 0.2534$, giving a new small region of stability. If we continue this family, this time on the left, another further period-doubling bifurcation appears, leading to a new and smaller stability zone. Thus, we have a self-similar chain of connected regions, more and more smaller, that are created due to a sequence of pitchfork and period-doubling bifurcations.

Figures 5 and 6 are presented just to illustrate some of the bifurcations on this problem, without doing a complete study of Hamiltonian bifurcations under symmetries, which is out of the scope of the present paper. We note that a complete classification of bifurcation orbits in the presence of one symmetry appears in [36], and with more symmetries in [37]. See also the extensive literature on this subject [33], [38]–[40]. In the plots on the left we show the OFLI2 plots of just the bounded regular regions on color scale, and on the right we present a schematic Poincaré section computed from the normal form of the different bifurcations. We suppose that the bifurcation occurs at the value of the parameter $\mathcal{P}_B$ and we write $\mathcal{P} = \mathcal{P}_B + \varepsilon$. Note that we only show one direction, from $\varepsilon < 0$ to $\varepsilon > 0$, but it could be the opposite depending on the particular bifurcation.

Figure 5 shows an example of generic bifurcations. In the picture on the left, we plot some families of symmetric periodic orbits on plane (y, E). It corresponds to the region of figure 4(B), but to illustrate the bifurcations we are interested in, we plot only some of the

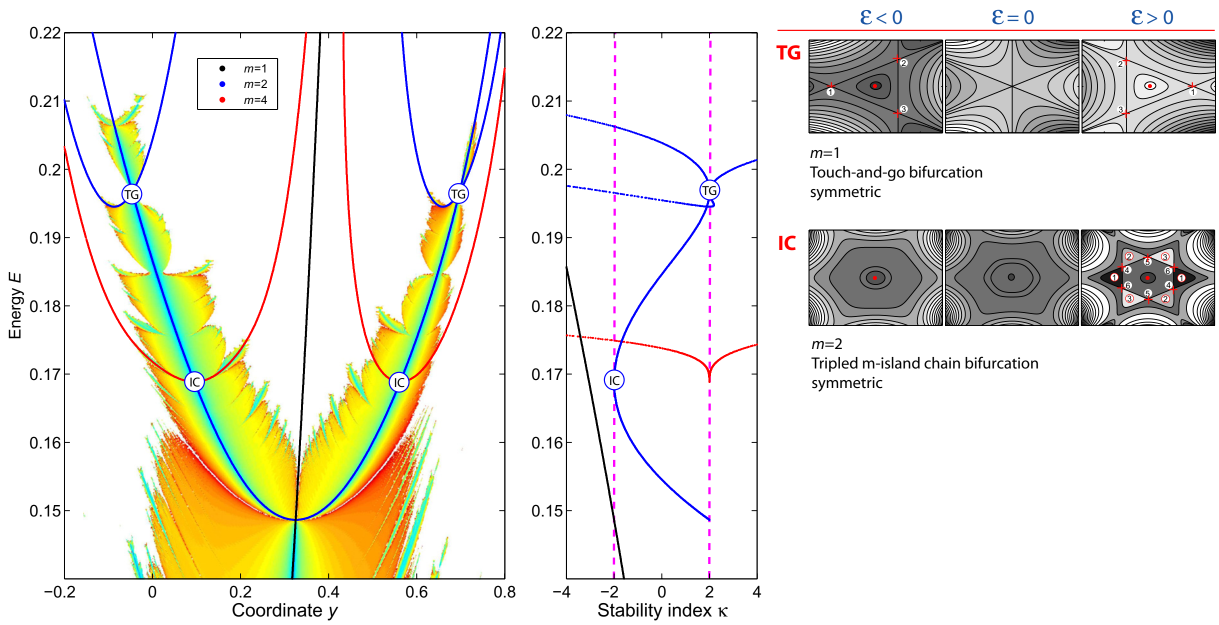

Figure 6. Non-generic bifurcations below the escape energy. On the left, both OFLI2 and families of periodic orbits of multiplicity 1 (Π_8), 2 and 4. The middle plot shows the stability index κ of these families. On the right, schematic Poincaré surface sections for two non-generic bifurcations.

families. In the middle figure, we show the stability index κ versus the energy E (left). The main family of multiplicity $m = 1$ is the one in black. The other families bifurcate from this on the points marked with a circle (points given by (5)). Note that the bifurcated families always begin with a value of $\kappa = 2$. This regular region above the escape energy E_e is also shown in figures 2(B), 3(E) and 3(F), and the main family of periodic orbits does not present D_3 symmetry. It appears with a saddle-node bifurcation (SN), which is a non-elementary periodic solution ($\kappa = 2$) and corresponds to the case where two periodic orbits are created (or destroyed), one stable and another one unstable. This is the only way of creating new families of periodic orbits, apart from the boundaries of the domain of definition of the Poincaré map. The stable branch changes its stability index until it reaches $\kappa = 2$ again, where an isochronous pitchfork bifurcation (P) appears. It is a symmetric pitchfork bifurcation: from a symmetric periodic orbit two new isochronous periodic orbits are created but with fewer symmetries (the symmetry in this case is on the y-axis, not D_3) and the main symmetric periodic orbit changes its stability character after the bifurcation. Besides, we plot the generic touch-and-go bifurcation, as an example of a known generic bifurcation [38] (and to compare it with the non-generic case explained later) where an unstable periodic orbit of multiplicity $m = 3$ touches the center $m = 1$ periodic orbit and 'bounces' while the main orbit remains stable. None of the orbits disappear.

Figure 6 shows some examples of non-generic bifurcations. Orbit Π_8 presents the D_3 symmetry, and the family of multiplicity $m = 2$ coming after a period-doubling generic bifurcation keeps the D_3 symmetry. However, the subsequent period-doubling giving birth to the family of multiplicity $m = 4$ is a non-generic bifurcation and due to the D_3 symmetry the resonant islands created around the main orbit are tripled and three unstable and stable periodic orbits appear (IC—tripled 2-period island chain). Besides, the main orbit, i.e. the $m = 2$ family, is still stable. Note that, just looking at the Poincaré surface of section, this bifurcation may be confused with a different island chain bifurcation, but, obviously, if you know the multiplicity of the different orbits involved there is no confusion at all. Later, there is an isochronous touch-and-go bifurcation: three unstable orbits of $m = 2$ collapse with the main family and then reappear again as unstable orbits with the Poincaré surface of section rotated. This is different from the generic version of this bifurcation described above. Note that there is another generic period-doubling (and so different from the IC described previously) for an energy value of about $E \simeq 0.207$ when the stability index $\kappa = -2$, but we have not drawn the family which arises from that bifurcation to avoid cluttering the figure.

5. Other systems with escapes

In the above sections, we have studied the HH potential as a paradigmatic example of open Hamiltonians, but the study is applicable to any 2DOF Hamiltonian system with escapes. In this section, we have chosen two other different Hamiltonians [9, 14, 41] with two and four escapes, such as:

$$\mathcal{H}_2 = \tfrac{1}{2}(X^2 + Y^2) + \tfrac{1}{2}(x^2 + y^2) - xy^2, \tag{6}$$

$$\mathcal{H}_4 = \tfrac{1}{2}(X^2 + Y^2) + \tfrac{1}{2}(x^2 + y^2) - x^2y^2. \tag{7}$$

These Hamiltonians present different symmetries from the HH Hamiltonian. The first Hamiltonian $\mathcal{H}_2$ is symmetric with respect to $y \mapsto -y$ and has two exits for values of the energy $E > 1/8$. Its potential is called the Barbanis potential in the chemistry community (just the potential) and it is extensively used in quantum dynamics [7] and to model $S_1 \leftarrow S_0$ fluorescence excitation of benzophenone [8]. The second Hamiltonian $\mathcal{H}_4$ is invariant under $x \mapsto -x$ or $y \mapsto -y$ and has four escapes for values of the energy $E > 1/4$. It is used in modeling galactic movements [14, 42].

In figure 7, we show combined OFLI2 and s.p.o. plots and exit basin plots for both Hamiltonians. Plots A and C belong to the equation (6) Hamiltonian and are drawn on the (x, E) plane, and plots B and D belong to equation (7) Hamiltonian and are drawn on the (y, E) plane. The color code is the same as for HH (since the equation (7) Hamiltonian has an extra escape, plot D uses cyan to indicate that additional exit). There is a correspondence between the several numeric methods as before. Since they do not have the same threefold symmetry as HH, we do not have those non-generic bifurcations. In this figure, we show instead some of the generic and y-axis symmetric bifurcations that we have previously shown in figure 5. We also remark that as occurs in the HH Hamiltonian, after the KAM regime there are small bounded regular regions originating from generic saddle-node bifurcations. This very interesting phenomenon is illustrated in the magnifications on the top, where we show the OFLI2 plot (now the main region of blue color indicates bounded regular orbits and the red color corresponds to transient unbounded chaotic orbits) and the main family of periodic orbits created on the bifurcation. Also, as occurs in the HH case, the normal modes behave as the organizing families of p.o. as all the other p.o. approach them and also configure the exit basin regions for large values of the energy.

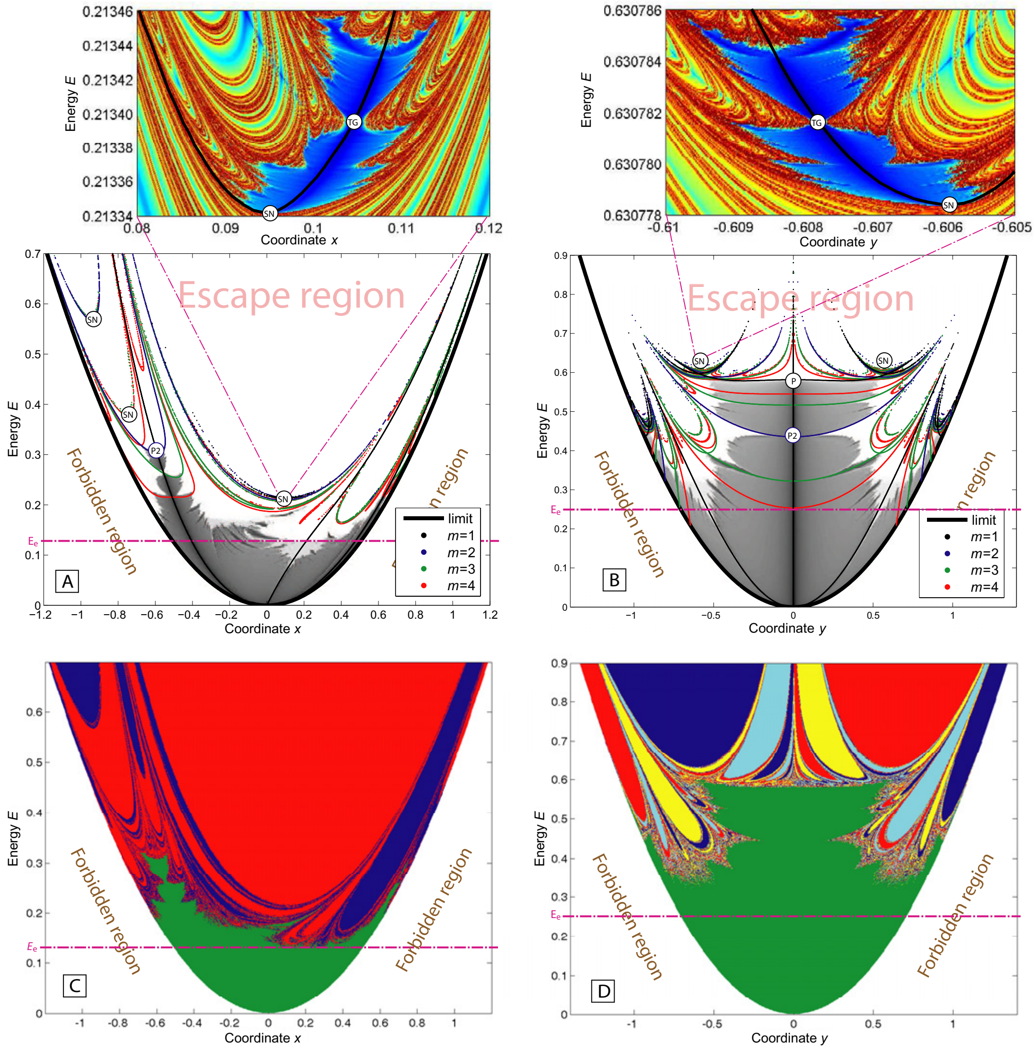

Figure 7. Combined s.p.o. and OFLI2 plots (A) and exit basins (C) on the (x, E) plane of the equation (6) Hamiltonian. Combined s.p.o. and OFLI2 plots (B) and exit basins (D) on the (y, E) plane of the equation (7) Hamiltonian.

6. Conclusions

The results presented here are of general interest in describing how the different kinds of orbits in open Hamiltonians are organized. Moreover, we have shown how two powerful numerical techniques, such as the OFLI2 chaos indicator [15] and a systematic search of s.p.o. [17, 21], provide us with two very useful tools: the location of the regular/chaotic orbits and the skeleton of periodic orbits. A careful combination of both techniques has been the key tool in detecting interesting phenomena in these systems. Note that without the combination of both tools some small regions of interest are completely undetectable.

We have seen that this kind of system has safe bounded regular regions of a significant size inside the escape region. Therefore, it is possible to find regions of nonzero measure with stable periodic or quasi-periodic orbits far from the KAM regime and far from the escape energy. So, these regions act as safe bounded regular regions inside the escape region, giving the only initial conditions of these systems that exhibit this behavior for large values of the energy. We have identified the mechanism of creation of these regions, the sudden appearance of chains of saddle-node bifurcations of periodic orbits that form regular regions near them. To locate these regions we need a highly precise skeleton of periodic orbits and a 2D plate of the OFLI2 chaos indicator (or any similar tool). We have illustrated this kind of region in the classical HH Hamiltonian, the Barbanis potential and a galactic Hamiltonian.

Moreover, we have shown that the simultaneous use of the OFLI2 and the skeleton of periodic orbits provides us with some descriptive plates, showing the organization of the regular regions around the families of periodic orbits and how the exit basins and the skeleton of s.p.o. are guided by the normal modes. Besides, we have obtained some special cases of bifurcations for the different symmetries of the systems. This is quite an interesting topic to extend the results of our work.

Acknowledgment

RB and SS have been supported by the Spanish Research Grant MTM2006-06961 and FB by the Spanish Research Grant AYA2008-05572/ESP.

References

[1] Aguirre J, Vallejo J C and Sanjuán M A F 2001 Wada basins and chaotic invariant sets in the Hénon–Heiles system *Phys. Rev.* E **64** 066208

[2] Aguirre J and Sanjuán M A F 2003 Limit of small exits in open Hamiltonian systems *Phys. Rev.* E **67** 056201

[3] Aguirre J, Viana R L and Sanjuán M A F 2009 Fractal structures in nonlinear dynamics *Rev. Mod. Phys.* **81** 333–86

[4] Kroetz T, Roberto M, da Silva E C, Caldas I L and Viana R L 2008 Escape patterns of chaotic magnetic field lines in a tokamak with reversed magnetic shear and an ergodic limiter *Phys. Plasmas* **15** 092310

[5] Horvath G Zs, Hernandez-Pozos J-L, Rink J, Dholakia K, Segal D M and Thompson R C 1998 Ion dynamics in perturbed quadrupole ion traps *Phys. Rev.* A **57** 1944

[6] Kawai S, Bandrauk A D, Jaffé C, Bartsch T, Palacián J and Uzer T 2007 Transition state theory for laser-driven reactions *J. Chem. Phys.* **126** 164306

[7] Babyuk D, Wyatt R E and Frederick J H 2003 Hydrodynamic analysis of dynamical tunneling *J. Chem. Phys.* **119** 6482–8

[8] Sepulveda M A and Heller E J 1994 Semiclassical analysis of hierarchical spectra *J. Chem. Phys.* **101** 8016–27

[9] Hénon M and Heiles C 1964 The applicability of the third integral of motion: some numerical experiments *Astron. J.* **69** 73–9

[10] Brack M, Kaidel J, Winkler P and Fedotkin S N 2006 Level density of the Hénon–Heiles system above the critical barrier energy *Few-Body Syst.* **38** 147–52

[11] Brack M, Mehta M and Tanaka K 2001 Occurrence of periodic Lamé functions at bifurcations in chaotic Hamiltonian systems *J. Phys. A: Math. Gen.* **34** 8199–220

[12] Fedotkin S N, Magner A G and Brack M 2008 Analytic approach to bifurcation cascades in a class of generalized Hénon–Heiles potentials *Phys. Rev.* E **77** 066219

[13] Barrio R, Blesa F and Serrano S 2008 Fractal structures in the Hénon–Heiles Hamiltonian *Europhys. Lett.* **82** 10003

[14] Kandrup H E, Siopis C, Contopoulos G and Dvorak R 1999 Diffusion and scaling in escapes from two-degrees-of-freedom Hamiltonian systems *Chaos* **9** 381–92

[15] Barrio R 2005 Sensitivity tools versus Poincaré sections *Chaos Solitons Fractals* **25** 711–26

[16] Barrio R 2006 Painting chaos: a gallery of sensitivity plots of classical problems *Int. J. Bifurcation Chaos Appl. Sci. Eng.* **16** 2777–98

[17] Barrio R and Blesa F 2009 Systematic search of symmetric periodic orbits in 2DOF Hamiltonian systems *Chaos Solitons Fractals* at press doi:10.1016/j.chaos.2008.02.032

[18] Birkhoff G D 1915 The restricted problem of three bodies *Rend. Circ. Mat. Palermo* **39** 265–334

[19] Strömgren E 1925 Connaissance actuelle des orbites dans le problème des trois corps *Bull. Astron.* **9** 87–130

[20] DeVogelaere R 1958 On the structure of periodic solutions of conservative systems, with applications *Contributions to the Theory of Nonlinear Oscillations* vol 4 (Princeton, NJ: Princeton University Press) pp 53–84

[21] Hénon M 1965 Exploration numérique du problème restreint. II. Masses égales, stabilité des orbites périodiques *Ann. Astrophys.* **28** 992–1007

[22] Hénon M 1969 Numerical exploration of the restricted problem. V. Hill's case: periodic orbits and their stability *Astron. Astrophys.* **1** 223–38

[23] Duarte P 1994 Plenty of elliptic islands for the standard family of area preserving maps *Ann. Inst. H Poincaré Anal. Non Linéaire* **11** 359–409

[24] Brack M 2001 Bifurcation cascades and self-similarity of periodic orbits with analytical scaling constants in Hénon–Heiles type potentials *Found. Phys.* **31** 209–32

[25] Arioli G and Zgliczyński P 2001 Symbolic dynamics for the Hénon–Heiles Hamiltonian on the critical level *J. Differ. Eqns* **171** 173–202

[26] Aguirre J, Vallejo J C and Sanjuán M A F 2003 Wada basins and unpredictability in Hamiltonian and dissipative systems *Int. J. Mod. Phys.* B **17** 4171–5

[27] Arioli G and Zgliczyński P 2003 The Hénon–Heiles Hamiltonian near the critical energy level—some rigorous results *Nonlinearity* **16** 1833–52

[28] Papadakis K, Goudas C and Katsiaris G 2005 The general solution of the Hénon–Heiles problem *Astrophys. Space Sci.* **295** 375–96

[29] Weinstein A 1973 Normal modes for nonlinear Hamiltonian systems *Invent. Math.* **20** 47–57

[30] Churchill R C, Pecelli G and Rod D L 1979 A survey of the Hénon–Heiles Hamiltonian with applications to related examples *Stochastic Behavior in Classical and Quantum Hamiltonian Systems* (*Lecture Notes in Physics* vol 93) (Berlin: Springer) pp 76–136

[31] Barrio R, Blesa F and Lara M 2005 VSVO formulation of the Taylor method for the numerical solution of ODEs *Comput. Math. Appl.* **50** 93–111

[32] Seoane J M, Aguirre J, Sanjuán M A F and Lai Y C 2006 Basin topology in dissipative chaotic scattering *Chaos* **16** 023101

[33] Meyer K R 1970 Generic bifurcation of periodic points *Trans. Am. Math. Soc* **149** 95–107

[34] Kurosaki S 1995 Detailed bifurcations of periodic orbits with threefold symmetry of the Hénon–Heiles Hamiltonian *J. Phys. Soc. Japan* **64** 3589–92

[35] Ozaki J and Kurosaki S 1995 Periodic orbits of Hénon–Heiles Hamiltonian—bifurcation phenomenon *Prog. Theor. Phys.* **95** 519–29

[36] Rimmer R J 1983 Generic bifurcations for involutory area preserving maps *Mem. Am. Math. Soc.* **41** 1165

[37] de Aguiar M A M, Malta C P, Baranger M and Davies K T R 1987 Bifurcations of periodic trajectories in nonintegrable Hamiltonian systems with two degrees of freedom: numerical and analytical results *Ann. Phys.* **180** 167–205

[38] Mao J M and Delos J B 1992 Hamiltonian bifurcation theory of closed orbits in the diamagnetic Kepler problem *Phys. Rev.* A **45** 1746–61

[39] Dellnitz M, Melbourne I and Marsden J E 1992 Generic bifurcation of Hamiltonian vector fields with symmetry *Nonlinearity* **5** 979–96

[40] Schomerus H 1998 Periodic orbits near bifurcations of codimension two: classical mechanics, semiclassics and Stokes transitions *J. Phys. A: Math. Gen.* **31** 4167–96

[41] Churchill R C, Pecelli G and Rod D L 1980 Stability transitions for periodic orbits in Hamiltonian systems *Arch. Ration. Mech. Anal.* **73** 313–47

[42] Contopoulos G 2002 *Order and Chaos in Dynamical Astronomy (Astronomy and Astrophysics Library)* (Berlin: Springer)